Large-area blown bubble films of aligned nanowires and carbon nanotubes

GUIHUA YU[1]*, ANYUAN CAO[2]*† AND CHARLES M. LIEBER[1,3]†

[1]Department of Chemistry and Chemical Biology, Harvard University, Cambridge, Massachusetts 02138, USA
[2]Department of Mechanical Engineering, University of Hawaii at Manoa, Honolulu, Hawaii 96822, USA
[3]Division of Engineering and Applied Sciences, Harvard University, Cambridge, Massachusetts 02138, USA
*These authors contributed equally to this work.
†e-mail: anyuan@hawaii.edu; cml@cmliris.harvard.edu

Published online: 27 May 2007; doi:10.1038/nnano.2007.150

Many of the applications proposed for nanowires and carbon nanotubes require these components to be organized over large areas with controlled orientation and density. Although progress has been made with directed assembly and Langmuir–Blodgett approaches, it is unclear whether these techniques can be scaled to large wafers and non-rigid substrates. Here, we describe a general and scalable approach for large-area, uniformly aligned and controlled-density nanowire and nanotube films, which involves expanding a bubble from a homogeneous suspension of these materials. The blown-bubble films were transferred to single-crystal wafers of at least 200 mm in diameter, flexible plastics sheets of dimensions of at least 225 × 300 mm^2 and highly curved surfaces, and were also suspended across open frames. In addition, electrical measurements show that large arrays of nanowire field-effect transistors can be efficiently fabricated on the wafer scale. Given the potential of blown film extrusion to produce continuous films with widths exceeding 1 m, we believe that our approach could allow the unique properties of nanowires and nanotubes to be exploited in applications requiring large areas and relatively modest device densities.

Semiconductor nanowires (NWs) and carbon nanotubes (NTs) exhibit physical properties that make them attractive building blocks for many electronic and optical applications[1–3]. To realize such applications, researchers have directed considerable effort to the development of methods of assembly that might ultimately lead to integrated systems. For example, there have been studies of individual or small numbers of NW and NT devices prepared by random deposition, electric field directed assembly[4], flow-assisted alignment[5], and selective chemical and biological patterning[6,7], and up to centimetre-scale assembly of NWs using the Langmuir–Blodgett technique[8]. However, it is still unclear whether these methods can be extended to large-scale assembly of NWs and NTs on both rigid and flexible substrates with controlled alignment and density.

Blown film extrusion is a well-developed process for the manufacture of plastic films in large quantities, which involves extruding a molten polymer and inflating it to obtain a balloon, which can be collapsed and slit to form continuous flat films with widths exceeding 1 m at rates in the order of 500 kg h^{-1} (refs. 9–11). We have applied this basic idea for the first time to the formation of nanocomposite films where the density and orientation of the NWs and NTs are controlled within the film. The basic steps in our approach (Fig. 1a) consist of (i) preparation of a homogeneous, stable and controlled concentration polymer suspension of NWs or NTs, (ii) expansion of the polymer suspension using a circular die to form a bubble at controlled pressure, P, and expansion rate, where stable vertical expansion is achieved using an external vertical force, F, and (iii) transfer of the bubble film to substrates or open frame structures.

BLOWN BUBBLE FILMS

To characterize key features of this method, we first focused on silicon NW blown-bubble films (BBFs), because Si NWs can be produced in high yield with uniform diameters and electronic properties[8,12]. Si NWs were covalently modified using 5,6-epoxyhexyltriethoxysilane, and then combined with an epoxy solution to yield stable and well-dispersed suspensions from 0.01–0.22 wt% (see Methods). Once the Si NW–epoxy suspension viscosity increased to 15–25 Pa s during polymerization, 0.5–1 g of the suspension was transferred uniformly onto the top surface of the die, and blown into a single bubble using a nitrogen flow (P = 150–200 kPa) that directed the expansion vertically at a rate of 10–15 cm min^{-1} (Fig. 1b,c). Stable vertical expansion was facilitated by an upward moving ring that kept the bubble centred over the die. We routinely produce bubbles with diameters greater than 25 cm and heights greater than 50 cm using this semi-automated process (see Methods). Larger dies and greater control of the expansion process should enable much larger diameter bubbles to be produced, in analogy to the bubbles of 1–2 m diameter produced during automated processing of homogeneous polymers[11].

The BBFs could be transferred to both rigid and flexible substrates during the expansion process. For example, two 150-mm silicon wafers were fixed in positions close to the central axis of the die/bubble (Fig. 1b), and the bubble expansion was then continued until it covered the entire wafer surfaces (Fig. 1c). Optical inspection of the Si NW-BBF transferred to a 150-mm

diameter wafer (Fig. 1d) showed that the transferred film is uniform over the entire substrate, and more generally, our studies show that 80–90% of the transferred films are defect free, although we observe small defects in some samples due to trapped gas during film transfer. Higher magnification dark-field optical images (insets, Fig. 1d), which resolve individual Si NWs within the transferred BBF, show that the Si NWs recorded from different areas of this large substrate are well aligned along the upward expansion direction of the bubble. Indeed, the angular deviation of the Si NWs is less than 10° over the entire 150-mm-diameter wafer and represents a very substantial advance over previous studies[4–8].

Excellent orientational alignment of Si NWs was observed for BBFs with different NW densities prepared from 0.01–0.22 wt% Si NW–epoxy suspensions (Fig. 2a–d). The alignment and relatively uniform separation reproducibly observed in our experiments are still not fully understood. Qualitatively, the shear stress associated with the suspension passing through the circumferential edge of the die could align the high aspect ratio nanowires in a polymer fluid along the principal direction of strain. This explanation is consistent with previous observations of shear-induced alignment of rod-like micro/nanostructures in fluid systems[5,13,14]. As the bubble expands primarily in the vertical direction, with a continuous supply of NW suspension from the top surface of the die, the orientation of the NWs in the BBFs should always follow the upward (longitude) direction, which is consistent with optical images. Expansion along a defined direction, as achieved in our approach, is crucial to obtain consistent alignment of NWs over large areas, and enables the overall orientation to be fixed in an absolute sense during transfer to a substrate, independent of high-resolution imaging.

There is a clear decrease in Si NW separation (centre-to-centre spacing) and increase in density in the transferred BBFs as the starting concentration increases from 0.01–0.22 wt% (Fig. 2e). We find that the NW separation can be varied over at least an order of magnitude from 50 ± 8 to 3.0 ± 0.6 μm as concentration increases from 0.01–0.22 wt%. Correspondingly, NW density increases from $4.0 \pm 0.6 \times 10^4$ to $4.0 \pm 0.5 \times 10^6$ cm^{-2} for these same samples. The separations/densities of Si NWs produced so far are relatively modest, but these values are still useful for some applications, such as nanoelectronic transistor arrays for biological/chemical sensing and displays. The plot of spacing versus wt% (Fig. 2e) shows saturation approaching a micrometre separation at higher Si NW concentrations. Our experiments suggest that this may be in part attributed to observed NW aggregation, although one also expects similar behaviour based on this physical process (that is, a two-dimensional layer of particles should have a (particle concentration)$^{-1/2}$ functional dependence). Hence, it will be interesting in the future to better optimize the surface chemistry to enable uniform higher wt% suspensions to be prepared. This would allow for data extending the separation (density) versus wt% curves, and thus test the separation limits achievable with this approach and also develop a firm understanding of these limits.

In addition, scanning electron microscopy (SEM) and transmission electron microscopy (TEM) images (see Supplementary Information, Fig. S1a,b) show that BBFs have a uniform thickness, typically 200–500 nm. This observed variation is primarily due to differences in suspension volume transferred to the die prior to expansion and the final size of the bubble, and should be reduced by further process optimization. The SEM and TEM images of transferred films (see Supplementary Information, Fig. S1c,d) also show that most of the Si NWs are at the outer surface (of the bubble) and thus close to the substrate. We attribute the observed NW distribution to a drift of the aligned NWs in the polymer fluid to the outer surface due to the pressure gradient between the inner and outer

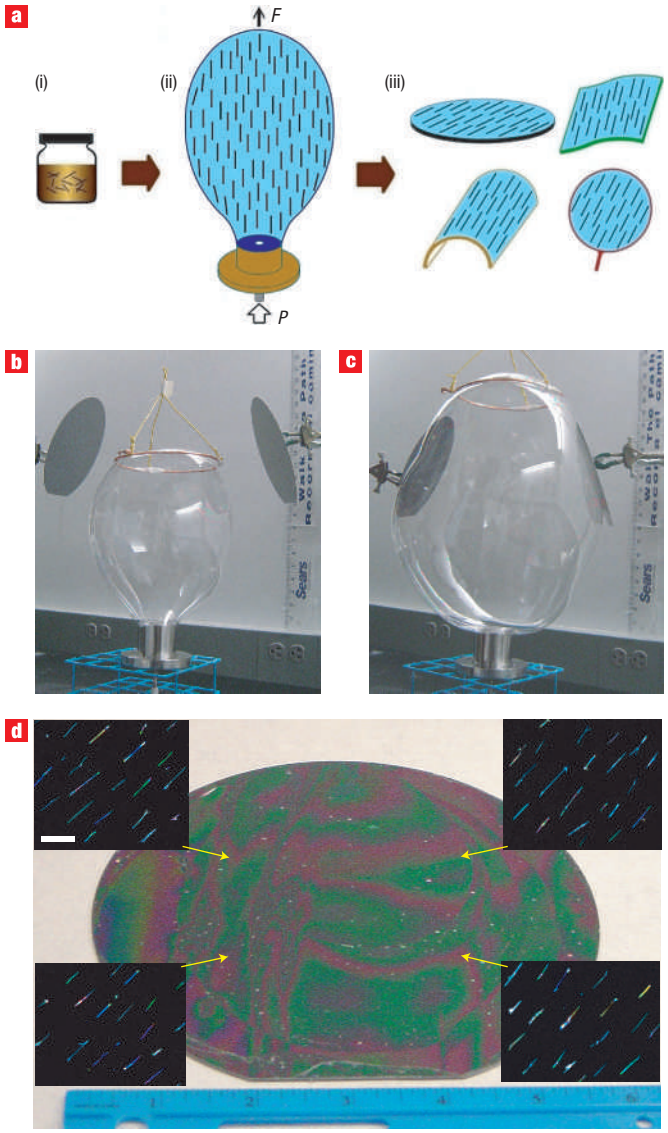

Figure 1 Blown bubble film (BBF) process. a, Illustration of (i) a NW/NT polymer suspension, (ii) bubble expansion over a circular die and (iii) films transferred to crystalline wafers, plastics, curved surfaces and open frames. In (ii), nitrogen gas at pressure *P* flows through the die and expands a bubble from the NW/NT-epoxy suspension (dark-blue colour) on the top of the die while a stable vertical force, *F*, is applied by means of a wire-ring connected to a controlled speed motor. Black straight lines represent aligned NWs/NTs embedded in the bubble film. **b**,**c**, Photographs of directed bubble expansion process at early and final stages, respectively. The ring visible at the top of the bubble moves upwards at a constant speed during expansion. In **c**, the BBF (bubble diameter 35 cm; height 50 cm) has coated the surface of two 150-mm silicon wafers. The range of the ruler behind bubble is 0–23 inches. **d**, Image of a 0.10 wt% Si NW-BBF transferred to a 150-mm Si wafer. Insets, dark-field optical images showing Si NWs in the film. The arrows point to the locations where the images were recorded. The orientation of the Si NWs corresponds to the upward expansion direction. The scale bar is 10 μm, and is the same in all insets.

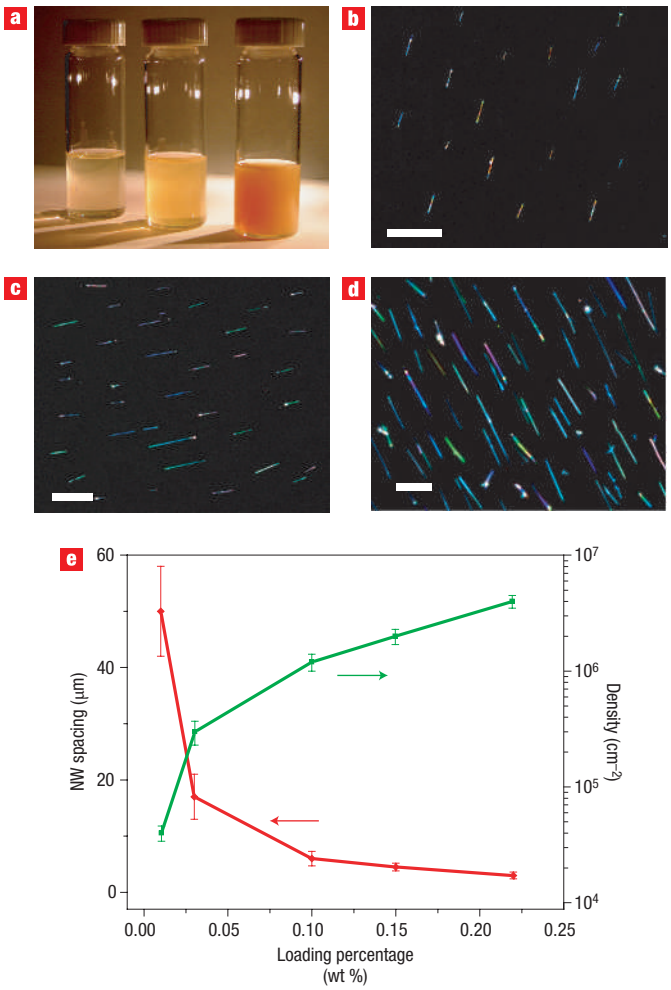

Figure 2 Control of aligned NW density in BBFs. a, Photograph of 0.01, 0.03 and 0.15 wt% (left to right) epoxy suspensions of Si NWs. **b–d**, Dark-field optical images recorded from 0.01 (**b**), 0.03 (**c**) and 0.15 (**d**) wt% Si NW-BBFs, respectively. The scale bars in **b**, **c** and **d** are 50, 20 and 10 μm, respectively. **e**, Plot of the average Si NW spacing and density as a function of the Si NW loading. Points were obtained from analysis of 3–8 independently prepared BBFs per wt% suspension.

walls. The drift velocity of NWs (toward the outer surface and along the normal of bubble curvature) and the distance travelled during bubble expansion can be estimated using the Faxen Laws[15], and are consistent with our observation of NWs at the outer bubble surface (see Supplementary Methods).

OTHER NANOWIRE AND CARBON NANOTUBE BBFs

We have explored the generality of this approach in terms of nanowire and nanotube materials, substrate structures and size scaling. For example, stable and homogeneous suspensions of the direct band-gap NW CdS were made and then used to prepare CdS NW-BBFs (see Methods). Optical images of transferred BBFs demonstrate uniform, well-aligned and controlled-density CdS NW with strong green emission (see Supplementary Information, Fig. S2). The ability to prepare aligned and controlled density arrays from different NWs should open up a number of opportunities for basic research and applications, given the distinct chemical and functional properties available from NW building blocks[1,16]. In addition, we modified single-walled NTs (SWNTs) and multiwalled NTs (MWNTs) with n-octadecylamine[17] and used the resulting suspensions to prepare BBFs (see Methods). The transferred SWNT- and MWNT-BBFs (Fig. 3a and b) show good alignment and uniformity over the 75-mm-diameter substrates used in the experiments, but can be transferred to much larger ones. The SWNTs exhibit an average separation of 1.5 ± 0.4 μm, and 90% are aligned to within 5° of the average orientation. The good alignment of the SWNTs within BBFs is notable in that their lengths, ~1–2 μm, are approximately ten times shorter than MWNTs (~20–25 μm) and Si NW (~10–15 μm) materials used in our studies. We also find that longer MWNTs, which are somewhat curled initially, appear straightened in the BBFs. The high degree of alignment for nanostructures with high aspect ratio can be understood within the framework of microhydrodynamics, in which the Péclet number, Pe, is estimated to be in the range of 10^3 to 10^6 ($\gg 1$) for the lengths of nanostructures studied here[15,18]. Sequential etching and SEM imaging also show that the NTs are, like the NWs, located at the outer ~60 nm of the BBFs, close to a two-dimensional layer, contrasting with NT composites made by solution casting or spin coating[19–21], which usually contain randomly oriented NTs through the thickness of the films.

BBFs ON LARGE-AREA AND NON-PLANAR SUBSTRATES

The BBF approach was also used to transfer aligned NW and NT films to a broad range of substrates. For example, a Si NW-BBF was transferred to a half cylinder (Fig. 3c), and subsequent dark-field optical images confirm that the NWs within the film are well aligned. We also note that NW- and NT-BBFs can be transferred to flexible plastic substrates that are subsequently bent into curved structures. In addition to planar and curved substrates, NW- and NT-BBFs have been transferred to open frames with good orientational alignment of the NW and NT materials (Fig. 3d), thus demonstrating the great flexibility of this approach.

Importantly, our approach has the potential to be scaled to structures of very large area[9–11]. A representative image of an SWNT-BBF transferred to a 200-mm wafer (Fig. 3e) shows that the film is remarkably uniform given the unsophisticated transfer process. Moreover, dark-field optical images (insets, Fig. 3e) demonstrate that the SWNTs have the same orientation and uniform separation across the diameter of this large substrate. Si NW-BBFs were also transferred uniformly, with good control of the Si NW alignment and density, to a large rectangular 225 mm × 300 mm plastic sheet substrate (Fig. 3f; see also Supplementary Information, Fig. S3). A histogram of angle distribution of over 400 Si NWs taken from different locations over the entire plastic substrate shows that more than 85% of the NWs are aligned within ±6° of the primary expansion/alignment direction.

LARGE-AREA TRANSISTOR ARRAYS

The high degree of alignment, controlled density and large area coverage possible with NW- and NT-BBFs could be enabling for a number of integrated electronics applications of these nanomaterials. To illustrate this potential, we have fabricated arrays of independently addressable NW-FETs from Si NW-BBFs transferred directly to 75-mm-diameter plastic substrates (see Methods). Figure 4a shows a 3 × 3 repeating transistor array, where each of the nine elements of the overall array consists of 400 independently addressable multi-NW transistors in a 20 × 20

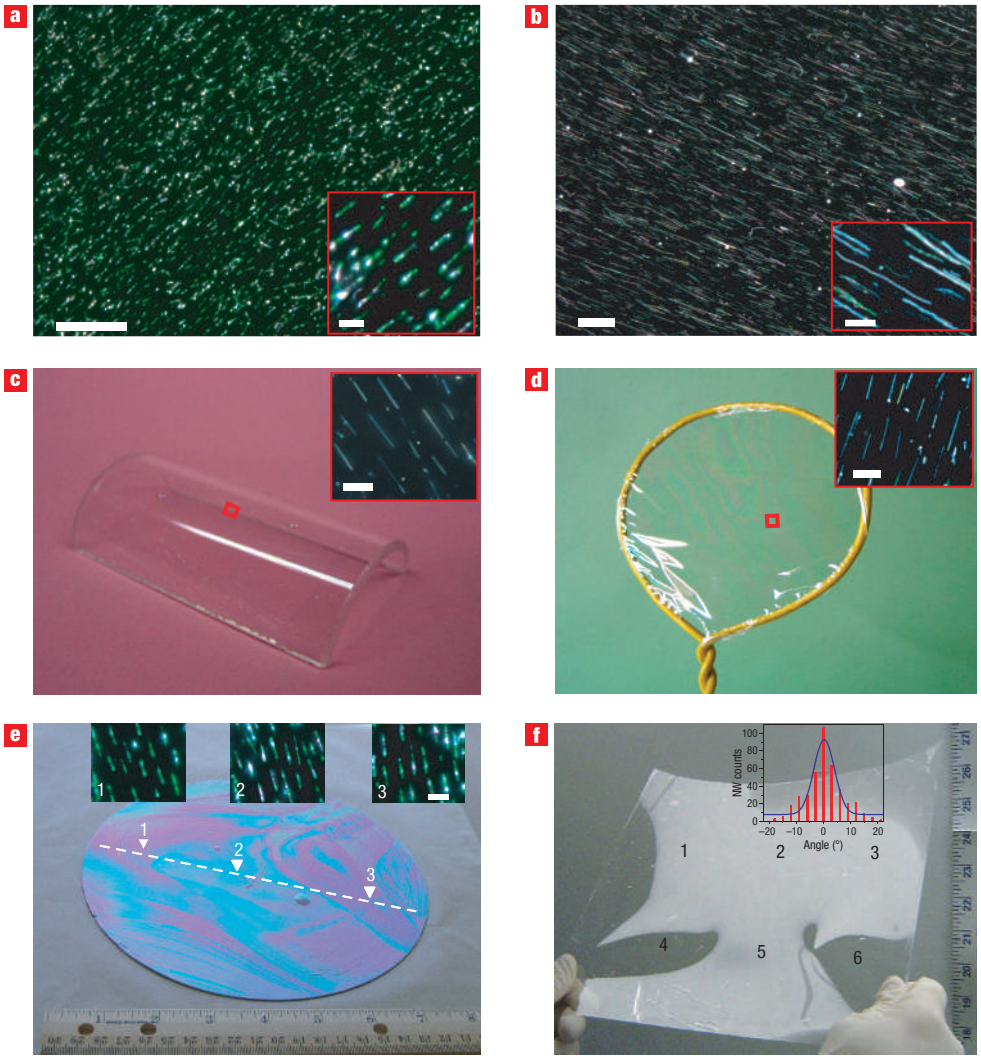

Figure 3 Versatility of BBFs. a, Dark-field optical image of a SWNT-BBF prepared from 0.07 wt% solution; the film was transferred to a silicon wafer for imaging. The scale bar represents 10 μm. Inset, high-resolution dark-field image highlighting the alignment of individual SWNTs; the scale bar is 2 μm. **b**, Dark-field optical image of an MWNT-BBF prepared from 0.15 wt% solution; the scale bar represents 25 μm. Inset, high-resolution image showing aligned, individual MWNTs; the scale bar is 5 μm. **c**, Image of a 0.10 wt% Si NW-BBF transferred to a curved surface (a half cylinder with diameter 2.5 cm and length 6 cm). Inset, dark-field optical image showing Si NWs in the film. The red rectangle in the main panel highlights the examined location and the scale bar is 10 μm. **d**, Image of a 0.10 wt% Si NW-BBF transferred to an open frame with diameter ~6 cm. Inset, dark-field optical image showing Si NWs in the film. The red rectangle highlights the examined location and the scale bar is 10 μm. **e**, Image of a 0.07 wt% SWNT-BBF transferred to a 200-mm Si wafer and its line-scanning alignment analysis. Insets: high-resolution dark-field images highlighting the alignment of SWNTs in the marked locations (triangles indicate recorded locations). The scale bar represents 2 μm, and is the same for all three insets. **f**, Image of a 0.10 wt% Si NW-BBF transferred to a 225 mm × 300 mm plastic substrate. Inset, histogram of angular distribution of >400 NWs from the regions marked with numbers 1–6. More than 85% of the NWs are aligned within ±6° of the upward expansion direction.

array (inset, Fig. 4a). The FETs (Fig. 4a, right) contain, on average, 12 Si NWs per device, although this number can be varied through changes in the wt% solution used for the BBF and the sizes of the contact electrodes.

Representative drain–source current, I_{ds}, versus gate voltage, V_g, data (Fig. 4b; see also Supplementary Information, Fig. S4) yield a peak transconductance, $g_m = dI_d/dV_g$, of 6 μS with an on current, I_{on}, of ~16 μA, an on/off ratio $>10^5$ and a threshold voltage, V_t, of 0.55 V. These values compare well with, or exceed, previous multi-Si NW FETs prepared using Langmuir–Blodgett assembly[8], and moreover, significant improvements should be possible, for example, by substituting much higher performance Ge/Si core/shell NWs[22]. Importantly, histograms of V_t and I_{on} (Fig. 4c and inset of Fig. 4b), show that these properties, critical to integrated systems, are well constrained, with values of 0.81 ± 0.32 V and 15.1 ± 3.7 μA, respectively. The good reproducibility of the Si NW FETs can be attributed to the uniform density, good alignment and preferential distribution of the NWs at a single surface of the BBFs (see Supplementary Information, Fig. S1), as this allows for the fabrication of repeatable device structures. The straightforward transfer of aligned Si NW-BBFs to large substrates makes this process considerably more efficient than previous fluid-directed[5] and Langmuir–Blodgett[8] assembly methods.

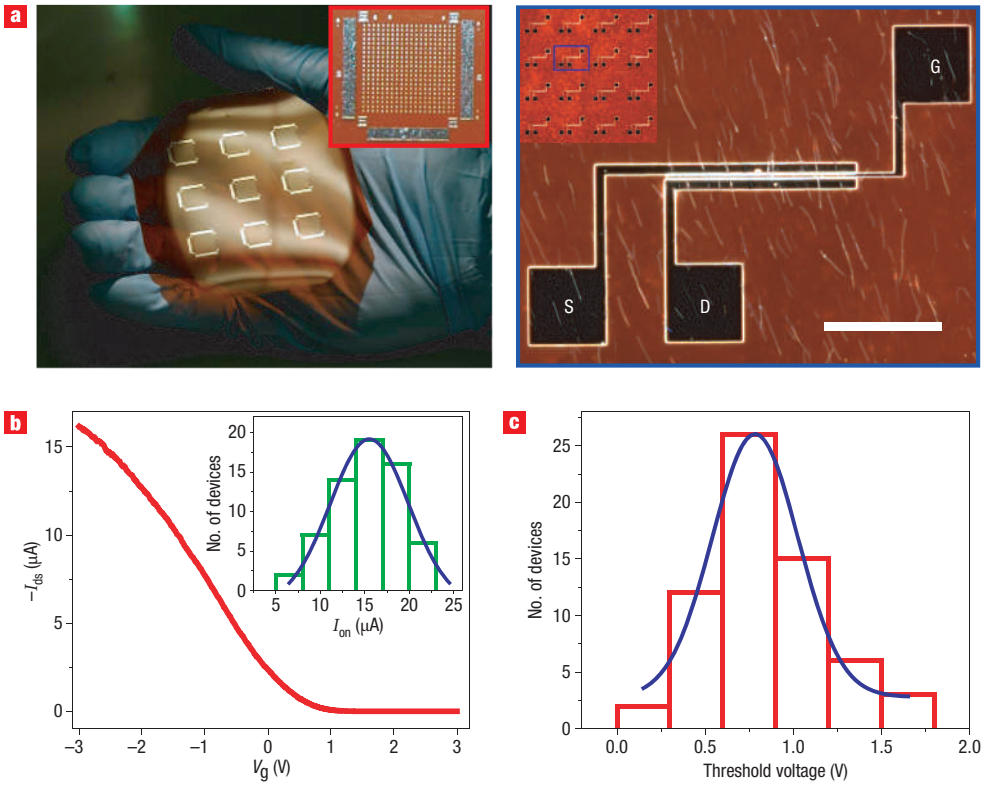

Figure 4 Si NW FET arrays on plastic substrates. a, Left panel, photograph of a plastic substrate containing nine Si NW-FETs device arrays. The device arrays were prepared by standard processing (see Methods) following transfer of the Si NW-BBF to the plastic. Inset, optical image of one device array from the centre of the substrate. Right panel, dark-field optical image of one typical top-gated Si NW-FET device; the scale bar represents 50 μm. Inset, optical image of a 4×4 Si NW FET subarray. The blue rectangle highlights a single device. **b**, Typical $I_{ds}-V_g$ characteristics of a 12-Si NW-FET device recorded with $V_{ds} = -1$V. Inset, histogram of I_{on} showing the uniform device characteristics, where the blue curve is a gaussian fit: 15.1 ± 3.7 μA. **c**, Histogram of threshold voltage determined from analysis of more than 60 randomly chosen devices in the larger array; the blue curve is a gaussian fit: 0.81 ± 0.32 V.

CONCLUSIONS

In summary, we have shown that bubble expansion of homogeneous NW and NT suspensions is a general approach for preparing well-aligned and controlled-density NW and NT films over large areas. In our work, we demonstrated these key features with NW- and NT-BBFs conformally transferred to single-crystal wafers up to 200 mm in diameter, flexible plastic sheets up to 225 mm × 300 mm, highly curved surfaces, and also suspended across open frames. We believe that the transfer of aligned and controlled-density NWs and NTs to both large crystalline wafers and flexible plastic substrates represents one of the most critical advances necessary for realizing many applications and/or efficient processing of these materials in several areas of electronics. In addition, our studies of large NW FET arrays fabricated from transferred Si NW-BBFs demonstrate that this approach yields devices with reproducible properties necessary for integrated electronics, although the modest density achieved to date makes them most applicable to areas such as biological/chemical sensors[23] and displays.

It remains a challenge for the future to see how far the density of aligned NWs and NTs can be pushed by our approach. More generally, we believe that these NW- and NT-BBFs should be scalable to much larger metre-scale sizes by controlling the steps of bubble formation and expansion as is currently achieved with homogeneous polymers[11], and moreover, that our approach could be extended to enable three-dimensional structures[24,25] produced by layering BBFs containing the same or distinct functional NWs and/or NTs, and by scrolling or folding the NW- and NT-BBFs. There are still challenges that must be addressed for our approach to reach the metre scale using established blown film extrusion techniques[9–11], including the development of a better understanding of the physics underlying alignment and spacing, and an understanding of the limits of matrix materials and properties.

METHODS

NW AND NT FUNCTIONALIZATION

The 20-nm-diameter p-type Si NWs were synthesized by chemical vapour deposition of silane and diborane with a Si:B ratio of 4,000:1 using gold nanoparticles (Ted Pella) as catalysts[8,12]. CdS NWs were prepared by thermal evaporation of CdS powder (Sigma-Aldrich) at the centre of a quartz reaction tube with subsequent NW growth on a substrate containing dispersed 30-nm gold nanoparticles located at the downstream edge of a furnace heated to 600 °C in 30 s.c.c.m. of H_2 at a total pressure of 30 torr. Si and CdS NW growth substrates were modified with 1% (v/v) 5,6-epoxyhexyltriethoxysilane (Gelest) in tetrahydrofuran (THF) for 2 h, rinsed with THF and cured at 110 °C for 10 min. The functionalized NWs were removed from growth substrates by sonication (60 W, 10 s). The mass of NWs used in suspension was determined from the difference in weight of the substrate before and after sonication.

SWNTs (P3-SWNT, purified SWNTs with high carboxylic acid content, Carbon Solutions) and MWNTs (produced by chemical vapour deposition, as described previously[26]) were modified with n-octadecylamine (ODA, Sigma-Aldrich). Briefly, 300 mg SWNTs were mixed with 2 g ODA and heated at 120 °C

for four days. The ODA-functionalized SWNTs were washed with ethanol and dried in air. SEM images show small bundles of ODA-SWNTs with lengths of ~2 μm. MWNTs (40 nm average diameter) were dispersed in 5 M nitric acid, heated at 110 °C to introduce carboxylic acid groups, and then isolated by filtration and washed with distilled water. Then 500 mg MWNTs were mixed with ODA (~2 g) and heated at 120 °C for 3–4 days. The ODA-functionalized MWNTs were washed with ethanol and dried in air.

PREPARATION OF NW AND NT SUSPENSIONS

Functionalized NWs (1–15 mg) or 5–20 mg ODA-SWNTs were suspended in 3–4 ml THF to obtain different wt% solutions. Then 5 g epoxy part A (FHI 3:1 HT Resin, Fiberglass Hawaii) was added to the THF solution, mechanically mixed (M37615 Mixer, Barnstead International) for 5 min, and 1.7 g epoxy part B (hardener) was added and the solution mixed for an additional 5 min. The resulting suspension was capped to prevent THF evaporation, and allowed to cure until the viscosity reached 15–25 Pa s (AR-2 rheometer, TA Instruments). During the first 10 h, suspensions were shaken every 2 h, and allowed to sit thereafter. Typically, 20–30 h were required before the suspensions reached the desired viscosity range.

SEMI-AUTOMATED PROCESS FOR PRODUCING BUBBLES

Controlled bubble expansion was carried out using an apparatus consisting of a 50-mm-diameter stainless steel die with a gas inlet (6.35 mm) at the bottom, an outlet (6.35 mm) at the top and a ring centred over the gas outlet, which was moved upward at a controlled speed. Rigid wafers and/or flexible substrates were set at fixed distances around the expansion axis. NW/NT suspensions (0.5–1 g) were transferred to the polished top surface of the die, forming a membrane covering the gas outlet, and then N_2 gas ($P = 150–200$ kPa) was introduced to initiate bubble expansion. The ring catches the top portion of the bubble and directs stable vertical expansion at an average speed of ~10–15 cm min^{-1}. Bubble films were transferred to wafer substrates during the expansion process.

NW-FET ARRAYS

Si NW-BBFs were transferred to 3-inch-diameter Kapton wafers (Kapton FPC polyimide film, DuPont) that were first coated with a ~1-μm-thick layer of cured photoresist (SU-8, MicroChem). Following oxygen reactive ion etching (Cirrus 150, Nexx Systems) to remove excess epoxy matrix, photolithography and metal deposition (50-nm Ni) were used to define source and drain electrodes. A ~20-nm HfO_2 dielectric was deposited over the wafer by low-temperature (110 °C) atomic layer deposition, and then gate electrodes were defined in a second photolithography and metal deposition (5-nm Cr; 50-nm Au) step. Devices were characterized at room temperature with a probe station (Summit 12561, Cascade Microtech) and semiconductor parameter analyser (4156 C, Agilent Technologies).

Received 13 February 2007; accepted 30 April 2007; published 27 May 2007.

References

1. Lieber, C. M. Nanoscale science and technology: building a big future from small things. *MRS Bull.* **28,** 486–491 (2003).
2. McEuen, P. L. Single-wall carbon nanotubes. *Phys. World* **13,** 31–36 (June 2000).
3. Avouris, P. Molecular electronics with carbon nanotubes. *Acc. Chem. Res.* **35,** 1026–1034 (2002).
4. Smith, P. A., Nordquist, C. D., Jackson, T. N. & Mayer, T. S. Electric-field assisted assembly and alignment of metallic nanowires. *Appl. Phys. Lett.* **77,** 1399–1401 (2000).
5. Huang, Y., Duan, X., Wei, Q. & Lieber, C. M. Directed assembly of one-dimensional nanostructures into functional networks. *Science* **291,** 630–633 (2001).
6. Auvray, S. *et al.* Chemical optimization of self-assembled carbon nanotube transistors. *Nano Lett.* **5,** 451–455 (2005).
7. Keren, K., Berman, R. S., Buchstab, E., Sivan, U. & Braun, E. DNA-templated carbon nanotube field-effect transistor. *Science* **302,** 1380–1382 (2003).
8. Jin, S. *et al.* Scalable interconnection and integration of nanowire devices without registration. *Nano Lett.* **4,** 915–919 (2004).
9. Briston, J. H. *Plastics Films* 71–86 (Longman Scientific & Technical, UK, 1989).
10. Quanbeck, J. *Plastics Machinery & Auxiliaries* 18 (May/June 2004).
11. Cantor, K. *Blown Film Extrusion: An Introduction*. (Hanser Gardner Publications, Cincinnati, 2006).
12. Cui, Y., Zhong, Z., Wang, D., Wang, W. U. & Lieber, C. M. High performance silicon nanowire field effect transistors. *Nano Lett.* **3,** 149–152 (2003).
13. Lin, M. Y. *et al.* Shear-induced behavior in a solution of cylindrical micelles. *Phys. Rev. E* **53,** R4302–R4305 (1996).
14. Hobbie, E. K., Wang, H., Kim, H., Lin-Gibson, S. & Grulke, E. A. Orientation of carbon nanotubes in a sheared polymer melt. *Phys. Fluids* **15,** 1196–1202 (2003).
15. Kim, S. & Karrila, S. J. *Microhydrodynamics: Principles and Selected Applications*, 1st edn, 76–128 (Butterworth–Heinemann, Boston, 1991).
16. Cui, Y., Duan, X., Huang, Y. & Lieber, C. M. *Nanowires and Nanobelts* (ed. Wang, Z. L.) 3–68 (Kluwer Academic/Plenum Publishers, Netherlands, 2003).
17. Chen, J. *et al.* Dissolution of full-length single-walled carbon nanotubes. *J. Phys. Chem. B* **105,** 2525–2528 (2001).
18. Bruinsma, R., Gelbart, W. M. & Ben-Shaul, A. Flow-induced gelation of living (micellar) polymers. *J. Chem. Phys.* **96,** 7710–7727 (1992).
19. Kilbride, B. E. *et al.* Experimental observation of scaling laws for alternating current and direct current conductivity in polymer–carbon nanotube composite thin films. *J. Appl. Phys.* **92,** 4024–4030 (2002).
20. Ounaies, Z., Park, C., Wise, K. E., Siochi, E. J. & Harrison, J. S. Electrical properties of single wall carbon nanotube reinforced polyimide composites. *Composites Sci. Technol.* **63,** 1637–1646 (2003).
21. Park, C. *et al.* Dispersion of single wall carbon nanotubes by in situ polymerization under sonication. *Chem. Phys. Lett.* **364,** 303–308 (2002).
22. Xiang, J. *et al.* Ge/Si nanowire heterostructures as high-performance field-effect transistors. *Nature* **441,** 489–493 (2006).
23. Patolsky, F., Timko, B. P., Zheng, G. & Lieber, C. M. Nanowire-based nanoelectronic devices in the life sciences. *MRS Bull.* **32,** 142–149 (2007).
24. Ahn, J. *et al.* Heterogeneous three-dimensional electronics by use of printed semiconductor nanomaterials. *Science* **314,** 1754–1757 (2006).
25. Javey, A., Nam, S. W., Friedman, R. S., Yan, H. & Lieber, C. M. Layer-by-layer assembly of nanowires for three-dimensional, multifunctional electronics. *Nano Lett.* **7,** 773–777 (2007).
26. Andrews, R. *et al.* Continuous production of aligned carbon nanotubes: a step closer to commercial realization. *Chem. Phys. Lett.* **303,** 467–474 (1999).

Acknowledgements

We thank M. Ghasemi-Nejhad and R.H. Knapp for helpful discussions. A.C. acknowledges start-up funding from Department of Mechanical Engineering and College of Engineering of University of Hawaii; C.M.L. acknowledges support of this work by Air Force Office of Scientific Research and Defense Advanced Research Projects Agency.
Correspondence and requests for materials should be addressed to A.C. and C.M.L.
Supplementary information accompanies this paper on www.nature.com/naturenanotechnology.

Author contributions

G.Y. and A.C. performed the experiments. G.Y., A.C. and C.M.L. designed the experiments, discussed the interpretation of results and co-wrote the paper.

Competing financial interests

The authors declare no competing financial interests.